This is a repository copy of *An ab initio investigation of alkali-metal non-covalent bonds B⬜LiR and B⬜NaR (R = F, H or CH3) formed with simple Lewis bases B : the relative inductive effects of F, H and CH3*.

White Rose Research Online URL for this paper:
https://eprints.whiterose.ac.uk/162383/

Version: Accepted Version

An *ab initio* investigation of alkali-metal non-covalent bonds B⋯LiR and B⋯NaR (R = F, H or CH₃) formed with simple Lewis bases B: The relative inductive effects of F, H and CH₃

Ibon Alkorta [a], J. Grant Hill [b] and Anthony C. Legon *[c,]

Abstract.

The alkali-metal bonds formed by simple molecules LiR and NaR (R = F, H or CH₃) with each of the six Lewis bases B = OC, HCN, H₂O, H₃N, H₂S and H₃P were investigated by *ab initio* calculations at the CCSD(T)/AVTZ and CCSD(T)/awCVTZ levels of theory with the aim of characterising this type of non-covalent interaction. In some complexes, two minima were discovered, especially for those involving the NaR. The higher-energy minimum (referred to as Type I) for a given B was found to have geometry that is isomorphous with that of the corresponding hydrogen-bonded analogue B⋯HF. The lower-energy minimum (when two were present) showed evidence of a significant secondary interaction of R with the main electrophilic region of B (Type II complexes). Energies D_e^{CBS} for dissociation of the complexes into separate components were found to be directly proportional to the intermolecular stretching force constant k_σ The value of D_e^{CBS} could be partitioned into a nucleophilicity of B and an electrophilicity of LiR or NaR, with the order $E_{\mathrm{LiH}} \gtrsim E_{\mathrm{LiF}} = E_{\mathrm{LiCH3}}$ for the LiR and $E_{\mathrm{NaF}} > E_{\mathrm{NaH}} \approx E_{\mathrm{NaCH3}}$ for the NaR. For a given B, the order of the electrophilicities is $E_{\mathrm{LiR}} > E_{\mathrm{NaR}}$, which presumably reflects the fact that Li⁺ is smaller than Na⁺ and can approach the Lewis base more closely. A SAPT analysis revealed that the complexes B⋯LiR and B⋯NaR have larger electrostatic contributions to D_e than do the hydrogen- and halogen-bonded counterparts B⋯HCl and B⋯ClF.

[a] *Instituto de Química Médica (IQM-CSIC), Juan de la Cierva, 3, E-28006 Madrid, Spain*
Email: ibon@iqm.csic.es

[b] *Department of Chemistry, University of Sheffield, Sheffield S3 7HF,UK.*
Email: grant.hill@sheffield.ac.uk

[c]*School of Chemistry, University of Bristol, Cantocks Close, Bristol BS8 1TS, U. K.*
Email: a.c.legon@bristol.ac.uk

1. Introduction.

The hydrogen bond has occupied a central role in chemistry and biology since it was first proposed in 1920 [1]. In recent years there has been an increased interest in other non-covalent interactions, with an accompanying proliferation of names such as the halogen bond, the tetrel bond, the pnictogen bond, and the chalcogen bond. Indeed, IUPAC has begun the task of providing definitions of these, with recommendations now published for hydrogen [2], halogen [3] and chalcogen [4] bonds. The essence of these definitions is that an electrophilic region associated with a hydrogen atom, a halogen atom or a chalcogen atom in a Lewis acid interacts with a nucleophilic region of a Lewis base. It is possible to generalise these definitions as follows [5]: We write a molecule containing an atom of an element E{g} belonging to Group g of the Periodic Table as E{g}–R, where R is the remainder of the molecule. If an electrophilic region is associated with an atom E{g}, then the non-covalent interaction of E{g}–R with a Lewis base B is written as B$\cdots$E{g}–R, where the three centred-dots $\cdots$ represent the interaction. Thus, a halogen bond is represented by B$\cdots$E{17}–R, a tetrel bond by B$\cdots$E{14}–R, and so on. The notation B$\cdots$E{1}–R signifies not only alkali metal bonds, for example a sodium bond R–Na$\cdots$B, but also formally includes the hydrogen bond R–H$\cdots$B.

The nature of the hydrogen bond has been the subject of some controversy. Some rules proposed many years ago [6,7] for predicting the angular disposition of the subunits H–R and B in the equilibrium geometry of B$\cdots$H–R were essentially electrostatic in origin. When the H–R molecule has the polarity $H^{\delta+}$–$R^{\delta-}$, it is assumed to lie along the local symmetry axis of a non-bonding (n) or a π bonding electron pair of B (the most nucleophilic region) , with the $H^{\delta+}$ atom acting as the most electrophilic region of H–R. A quantitative electrostatic version proposed by Buckingham and Fowler [8] was successful, but met with some opposition [9]. The ubiquity and uniqueness and hydrogen bonds are generally accepted to result from the fact that there are many molecules H–R of polarity $H^{\delta+}$–$R^{\delta-}$, in which the $H^{\delta+}$ atom is partially depleted of its single 1s electron. Therefore $H^{\delta+}$–R^{δ} can approach the most nucleophilic region of B (along the axis of the n- or π-electron pair) more closely than can, for example, $Cl^{\delta+}$–$R^{\delta-}$, before exchange repulsion becomes dominant.

The fact that the Li atom has the electronic configuration $1s^2\,2s^1$, has a single 2s electron and differs from H only by virtue of the $1s^2$ filled inner core of electrons invites a comparison of the hydrogen bond with its lithium bond analogue. As a result, there exists an extensive

literature of the lithium bond. It was fist investigated theoretically by Kollman, Liebman and Allen [10] in 1970 via *ab initio* calculations and was identified experimentally by Ault and Pimentel in 1975 [11] by means of matrix isolation spectroscopy. The early history of this non-covalent interaction has been reviewed by Scheiner in Chapter 6 of the book entitled 'Lithium Chemistry: A theoretical and experimental overview'[12]. Since then there has been significant (predominantly theoretical) interest in the lithium bond, as exemplified by refs. [13-24].

It is known [25] that sodium chloride and other simple compounds of sodium in the vapour phase at low pressure exist as ion-pair species, *i.e.* the contribution of Na^+Cl^- to the valence-bond description of the molecule is very close to 100%. The same is true when the alkali metal atom is potassium or rubidium. The percentage ionic character of the lithium halides in the vapour is lower, but still high at about 95% [25]. It is of interest to investigate pairwise interactions of LiR and NaR with Lewis bases B to give isolated complexes B···LiR and B···NaR, where R is an atom or simple group of atoms. A convenient way to do this is through good quality *ab initio* calculations.

We report here the results of *ab initio* calculations using the coupled cluster with single, double and perturbative triple excitations [CCSD(T)] method [26] and diffuse augmented triple-zeta correlation consistent basis sets, with extrapolation to the complete basis set (CBS), the aim of which is to determine the geometries and dissociation energies for two series of complexes B···LiR and B···NaR, where R is F, H or CH_3 and the Lewis bases B are CO, PH_3, H_2S, HCN, H_2O and NH_3. The Lewis bases were chosen for their simplicity and because they all carry non-bonding electron pairs as their most nucleophilic region. The Lewis acids LiR and NaR were also chosen for their simplicity. By varying R from H to F to CH_3 we seek to discover how the properties of B···LiR and B···NaR change when R has different inductive effects. Ingold [27] defined the inductive effect (symbol $\pm I$) as an electron-pair displacement (arising from unequal sharing of electron pairs between unlike atoms) that can be propagated along a chain of bound atoms by a mechanism of electrostatic induction, with the proviso that all displaced electron pairs remain bound in their original octets/duplets. When R = F, a $-I$ inductive effect (electron withdrawing from Na relative to R = H) is expected, but when R = CH_3 a $+I$ effect might occur (electron movement towards Na relative to R = H). Previously [28], [29], we have shown how the equilibrium dissociation energy D_e for the processes B···HX

= B + HX and B$\cdots$XY = B + XY (X and Y are halogen atoms) may be partitioned to provide a nucleophilicity N_B of B and an electrophilicity E_A of HX or XY. In the present article, this approach is tested for the indicated set of lithium (B$\cdots$LiR) and sodium (B$\cdots$NaR) non-covalent bonds. Another question to be answered is: How does the introduction of (1) a filled $1s^2$ shell of electrons into the electrophilic atom when changing from hydrogen-bonded complexes B$\cdots$HX to lithium-bonded complexes B$\cdots$LiR and (2) the addition of a filled $2s^2$ electron shell when further changing to sodium-bonded complexes B$\cdots$NaR affect their properties? In addition, symmetry adapted perturbation theory (SAPT) analyses have been carried out to assess the contribution of electrostatic, induction, exchange repulsion and charge transfer to the lithium and sodium non-covalent bonds and the results compared with those of related hydrogen-bond and halogen- bond systems.

2.   Theoretical Methods

2.1   Geometry optimisations and calculation of intermolecular stretching force constants k_σ

The geometries of the complexes have been optimised at the CCSD(T) level with, unless otherwise noted, the aug-cc-pVTZ (abbreviated as AVTZ) basis set [30-33]. To obtain more accurate energies, extrapolation to the CBS limit has been carried out. For the Hartree-Fock (HF) reference energies the HF/aug-cc-pVnZ//CCSD(T)/AVTZ (n = D, T, Q) energies were extrapolated using an exponential extrapolation [34], while the CBS limit correlation energy was estimated as CCSD(T)/aug-cc-pVn`Z//CCSD(T)/AVTZ ($n$` = T, Q), again using an exponential extrapolation. Finally, the dissociation energy was obtained as the difference between the total CBS energies of the monomers and the complex. All the HF and CCSD(T) calculations have been performed with the MOLPRO 2012 program [35].

Correlation of the outer-core electrons can have a large effect on the calculated properties of alkali metal containing systems, [33,36-38] particularly when the energy gap between the core and valence electrons becomes small. To probe the importance of correlating the 2s2p outer-core in sodium non-covalent bonds, the calculations were repeated using the weighted core-valence correlating basis aug-cc-pwCVTZ for sodium [33], with the aug-cc-pVTZ basis and default frozen-core approximation applied for all other elements. This combination shall be referred to as awCVTZ herein, and was also used in estimating the CBS limits. In the case of lithium, the 1s core orbital is significantly lower in energy than the valence

orbitals, and initial test calculations indicated that including this 1s orbital in the correlation treatment had a negligible effect on equilibrium geometries and interaction energies, in agreement with previous reports [39].

The *ab initio* calculations of k_σ were conducted at the CCSD(T)/AVTZ and CCSD(T)/awCVTZ levels of theory. The energy at the equilibrium geometry was first obtained and the energy $E(r)$ was then calculated for several fixed values of the intermolecular distance r in 2.5 pm increments about the equilibrium value r_e, with optimisation in all internal coordinates but r. The curve of $E(r - r_e)$ as a function of $(r - r_e)$ was fitted as a third-order polynomial in $(r - r_e)$ and the second derivative evaluated at $r = r_e$ to yield $k_\sigma^{exp} = \left(\frac{\partial^2 E(r)}{\partial r^2}\right)_{r=r_e}$

2.2   Effect of sodium outer-core correlation

Correlating the 2s2p on Na produces a relatively significant contraction of the B⋯Na–R intermolecular distance, typically around 0.04 – 0.05 Å. With H_2O as the Lewis base this contraction becomes even larger, reaching a maximum of 0.199 Å for H_2O⋯$NaCH_3$, which demonstrates the importance of accounting for this outer-core correlation in geometry optimisations. There is also a shortening of the Na–R bond within the sodium bond donor, which is contracted by around 0.03 to 0.07 Å. Logically, the decrease in the intermolecular distance is accompanied by an increase in the dissociation energy, with the largest effects observed with H_2O as the Lewis base. This effect reaches a maximum for H_2O⋯NaF, where the interaction is strengthened by 7.06 kJ mol^{-1}.

2.3   Symmetry-Adapted Perturbation Theory (SAPT) calculations.

The Psi4 V.1.2 program [40] was used to carry out SAPT [41,42] calculations at the SAPT2+(3)δMP2/aug-cc-pVTZ level on the CCSD(T) geometries. For brevity, this will be referred to as simply SAPT herein. The SAPT calculations involving sodium included the 2s2p outer-core in the correlation treatment and used the aug-cc-pwCVTZ basis, all other elements retained the standard frozen-core approximation. The chosen SAPT model chemistry includes a correction based on the supermolecular MP2 interaction energy, which has been shown to be

important for complexes that are electrostatically dominated [43], and this level of SAPT has been recommended as a "gold standard" for the calculation of noncovalent interaction energies[43]. Density fitting and MP2 natural orbital approximations were used in all SAPT calculations, and the individual SAPT terms were grouped into electrostatic, exchange, induction and dispersion components of the total interaction energy, using the so-called "chemist's grouping".[44]
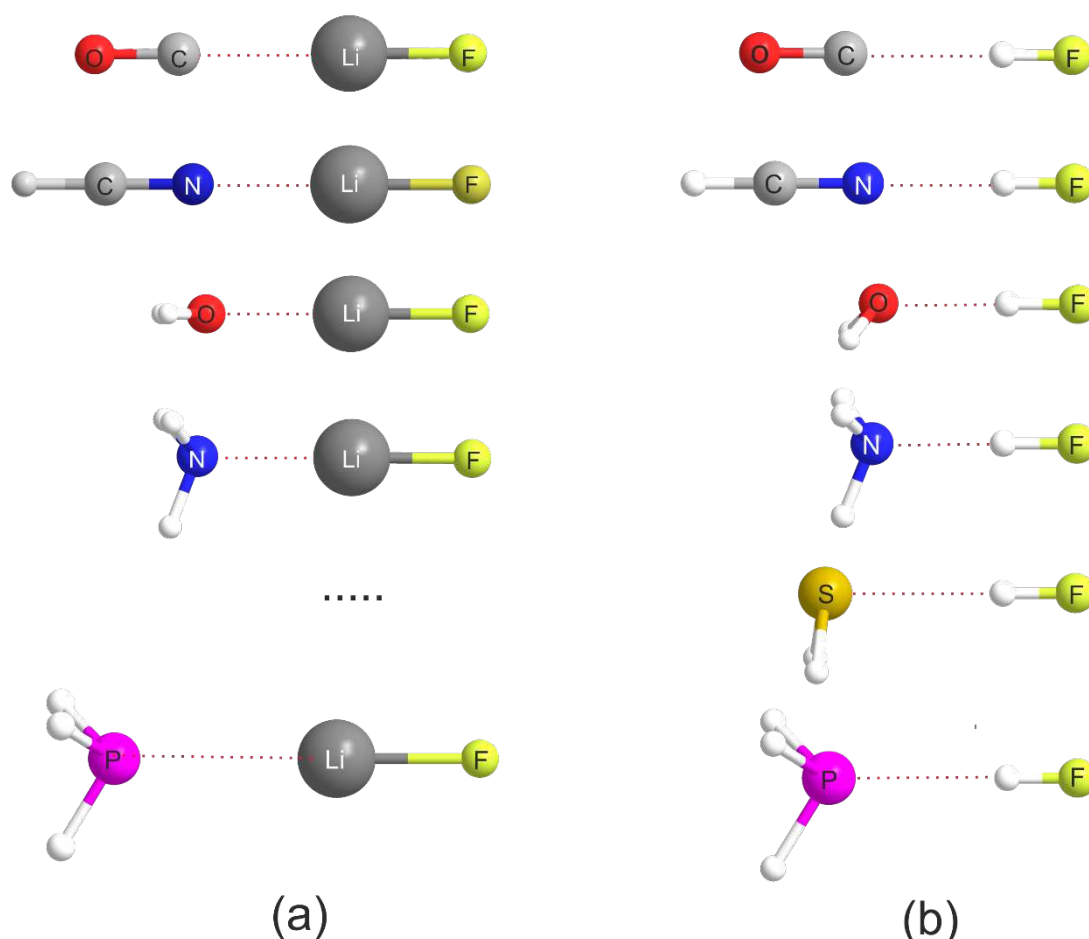
3 Results

3.1 Geometry of complexes

Figure 1. Optimised geometries of (a) the B···LiF complexes, where B = CO, HCN, H_2O, PH_3 and NH_3 and (b) the corresponding complexes of B···HF. Note that no minimum was found for H_2S···LiF

The optimised geometries of the B···LiF complexes, where B = CO, HCN, H_2O, PH_3 and NH_3 are shown drawn to scale in Figure 1(a). Only one energy minimum was found in each case, except H_2S···LiF for which no minimum was located. Quantitative details

(Cartesian coordinates and some internal coordinates of these geometries are available in Supplementary Material, Tables S1-S3. Also shown in Figure 1(b) for comparison are the corresponding geometries for the complexes B···HF optimised at the CCSD(T)/aug-cc-pVTZ level (as available from ref. [29]). We note from Figure 1 that for, a given B, the complex B···LiF is isomorphous with the corresponding B···HF complex. This appears at first glance not to be the case for H_2O···LiF and H_2O···HF but it is known that the potential energy barrier to inversion of the configuration at O in the latter molecule is only 1.5(8) kJ mol^{-1} [45], which is small in terms of the accuracy of *ab initio* energy calculations when comparing different systems. Certainly, both complexes are planar in the zero-point state and then have C_{2v} symmetry.

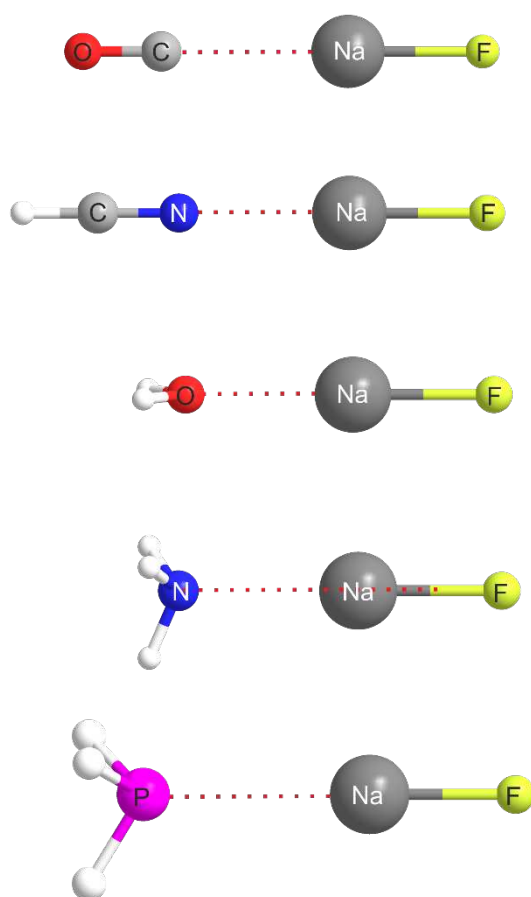Calculations for B···LiH and B···LiCH$_3$ reveal only one energy minimum in each case,

Figure 2. Type I complexes of B···NaF. The geometry of OC···NaF is that at the single minimum detected. For the remaining complexes two minima were detected and the geometries displayed pertain to the higher energy of the two minima.

which are associated with geometries that are isomorphous with those of B···LiF. The only exception is H_2O···LiH, for which two minima were located and only that of higher energy has

a geometry isomorphous with $H_2O \cdots LiF$. Quantitative details (cartesian coordinates and some internal coordinates) of these geometries are also available in Supplementary Material, Tables S1-S3. See below for discussion of the geometry at the lower energy minimum of $H_2O \cdots LiF$.

Calculations for $B \cdots NaF$ complexes using the weighted core-valence correlating basis aug-cc-pwCVTZ for sodium and the aug-cc-pVTZ basis for other atoms revealed two minima for $H_2O \cdots NaF$, $H_3N \cdots NaF$, $HCN \cdots NaF$ and $H_3P \cdots NaF$ while only a single minimum could be located for $H_2S \cdots NaF$ and $OC \cdots NaF$. The geometries at higher-energy minima of $B \cdots NaF$ (B $= H_2O$, H_3N, HCN and H_3P) and the single-minimum geometries for B $= H_2S$ and CO are displayed in Figure 2, from which it is clear that these geometries are isomorphous with those of the $B \cdots HF$ shown in Figure 1 and therefore that these geometries (as well as those of all $B \cdots LiF$ and $B \cdots LiCH_3$ and all but one of $B \cdots NaH$) are predicted by the rules [6,7] mentioned earlier. We shall refer to those geometries that are isomorphous with those of $B \cdots HF$ shown in Figures 1 and 2 as Type I geometries, whether they occur at a single minimum or at the higher

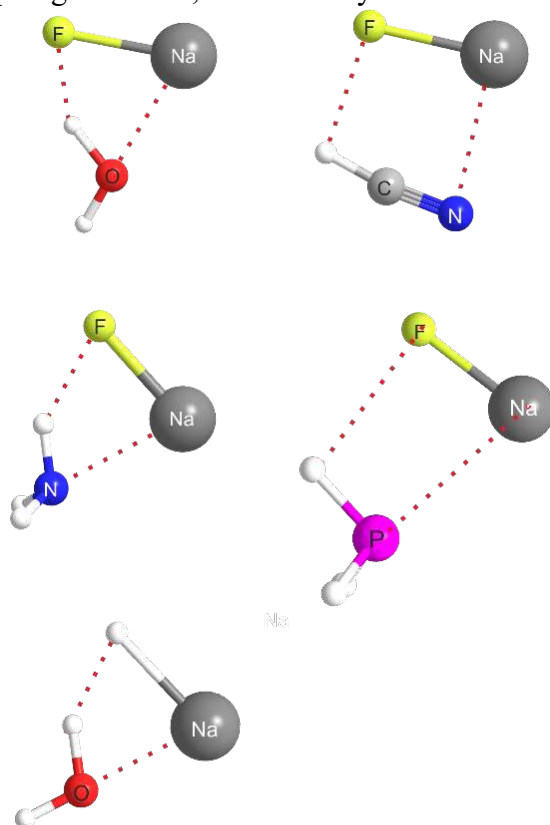Figure 3. Type II complexes of NaF and NaH with various Lewis bases B. The primary interaction is between Na and the non-bonding electron pair on the acceptor atom of B in each case. Secondary interactions occur between the H atoms of the Lewis base and either F or H of NaR.

8

energy minimum when two minima are detected. On the other hand, the lower energy geometries of B$\cdots$NaF when B = H$_2$O, H$_3$N, HCN and H$_3$P, and H$_2$O$\cdots$NaH, are clearly not isomorphous with those of B$\cdots$HF, as may be seen from the scale diagrams of these molecules collected in Figure 3

If the interaction of Na (the main electrophilic region of NaF) with a non-bonding electron pair of B in called the primary interaction, then the geometries at these lower-energy minima show strong evidence of a secondary interaction. The second non-covalent bond occurs between the most nucleophilic region of NaF or NaH (i.e. the region near the F or H atoms, respectively) and the most electrophilic region of B (usually a hydrogen atom) and is indicated by the usual dotted (red) line in Figure 3. Such lower energy complexes that are not isomorphous with the corresponding B$\cdots$HF are referred to as Type II complexes in what follows. If the higher energy Type I B$\cdots$NaF (or B$\cdots$NaH) complex is envisaged to form first, then we can imagine that the nucleophilic region at F (or H) seeks the electrophilic H atoms of B and the primary intermolecular bond bends until the lower energy minimum is achieved. This is an entirely formal view and is not a postulated mechanism. In addition to minima of the Type I and II, the linear complexes NaF$\cdots$HCN, LiF$\cdots$HCN, NaH$\cdots$HCN and LiH$\cdots$HCN stabilized by hydrogen bonds (F$\cdots$H in the first two and H$\cdots$H the last two) have been found. The D_e values for these complexes are 66.31, 51.74, 38.28 and 35.61 kJ mol^{-1}, respectively. Note that H$\cdots$H hydrogen-hydrogen bonds have been identified in earlier work [46].

3.2 Relationship between D_e and k_σ

Dissociation energies D_e for the process B$\cdots$MR = B + MR (M = Li or Na; R = F, H or CH$_3$) were calculated for complexes in which B = CO, HCN, H$_2$O, NH$_3$, H$_2$S and PH$_3$ at the CCSD(T)/CBS level, as described in Section 2.1. Energy minima were not located for H$_2$S$\cdots$LiF and H$_2$S$\cdots$NaF. The intermolecular stretching force constant k_σ is another measure given for B$\cdots$LiR in Table 1 while those for B$\cdots$NaR are given in Table 2, which includes values when using both the standard basis and frozen core [CCSD(T)/AVTZ] and CCSD(T)/awCVTZ. of binding strength; it is the restoring force accompanying infinitesimal displacement along the coordinate that leads eventually to the products B and MR. Calculation of k_σ values for the Type I complexes were carried out as described in Section 2.2. The results for D_e and k_σ are given for B$\cdots$LiR in Table 1 while those for B$\cdots$NaR are given in Table 2,

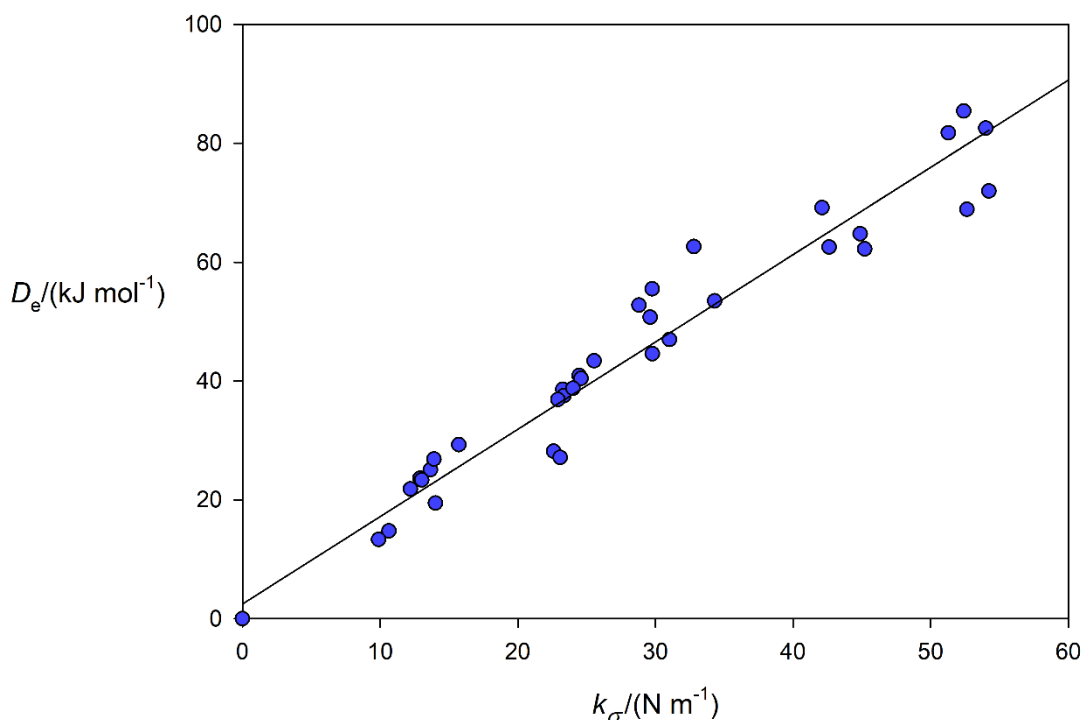which includes values when using both the standard basis and frozen core [CCSD(T)/AVTZ] and CCSD(T)/awCVTZ.

Figure 4. A graph of D_e versus k_σ for the series of Type I complexes B$\cdots$NaF, B$\cdots$NaH, B$\cdots$NaCH$_3$, B$\cdots$LiF, B$\cdots$LiH wih B = CO, HCN, H$_2$O, NH$_3$, H$_2$S and PH$_3$.

It has been shown elsewhere [28,29] that for many hydrogen-bonded complexes B$\cdots$HX (X is a halogen atom) and halogen-bonded complexes B$\cdots$XY (Y is a halogen atom) D_e is directly proportional to k_σ. Does such a relationship hold for the alkali-metal bonded complexes B$\cdots$LiR and B$\cdots$NaR (R = F, H and CH$_3$)? Figure 4 shows a plot of D_e(CBS) versus k_σ for the complexes B$\cdots$LiF, B$\cdots$LiH, B$\cdots$CH$_3$, B$\cdots$NaF, B$\cdots$NaH and B$\cdots$NaCH$_3$, when B = CO, HCN, H$_2$O, NH$_3$, H$_2$S and PH$_3$. Only type I complexes are chosen for this graph since these involve only one non-covalent interaction and are isomorphous with hydrogen- and halogen-bonded complexes B$\cdots$HX and B$\cdots$XY. The concepts of an intermolecular stretching force constant and the dissociation coordinate are more complicated for the NaR Type II complexes.

In Figure 4, the origin is taken as a point because when the value of D_e is zero there is no resistance to intermolecular stretching. The linear regression fit to the points in Figure 4 is

$$D_e = 1.47(5) \times 10^3 \text{ m}^2 \text{ mol}^{-1} \, k_\sigma + 2.5(15) \text{ kJ mol}^{-1}$$

when D_e and k_σ have units of kJ mol^{-1} and N m^{-1}, respectively, with $R^2 = 0.9485$. Figure 5 shows the corresponding plot for the hydrogen- and halogen-bonded complexes B$\cdots$HF, B$\cdots$HCl, B$\cdots$F$_2$, B$\cdots$Cl$_2$ and B$\cdots$ClF with the same set of B. The values of D_e(CBS) and k_σ for these complexes are taken from ref.[28]. The linear regression fit appropriate to Figure 5 is

$$D_e = 1.39(6)\, k_\sigma \times 10^3\ m^2\ mol^{-1} + 0.07(79)\ kJ\ mol^{-1} \quad with\ R^2 = 0.9660.$$

It appears therefore that there is a direct proportionality between D_e and k_σ for the B$\cdots$NaR and B$\cdots$LiR complexes included in Figure 4. This has implications for the radial potential energy functions for these complexes (see ref. [28] for a discussion). Moreover, the fact that the gradients of the linear regression fits shown in Figures 4 and 5 are identical within experimental error suggests that the same type of function could be used to describe the variation in potential energy with the intermolecular dissociation coordinate for both sets of complexes.
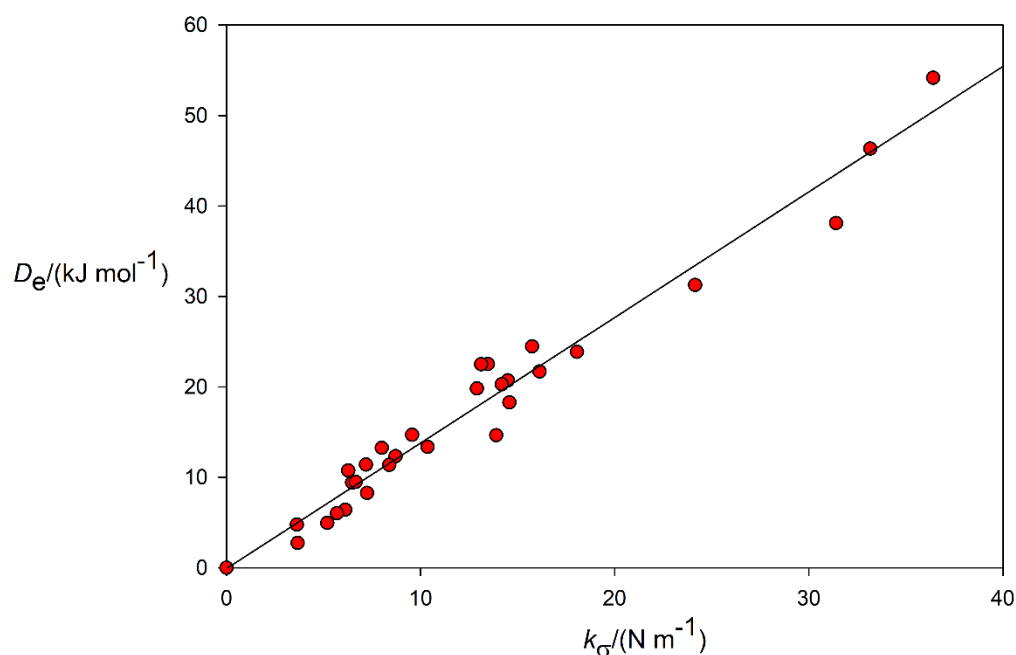

Figure 5. A plot of D_e versus k_σ for the series of complexes B$\cdots$HF, B$\cdots$HCl, B$\cdots$F$_2$, B$\cdots$Cl$_2$ and B$\cdots$LiH for B = CO, HCN, H$_2$O, NH$_3$, H$_2$S and PH$_3$. Data are from ref. [28].

3.3 Electrophilicities of LiR and NaR (R =F, H or CH$_3$) and nucleophilicities of B

Dissociation energies D_e calculated at the CCSD(T)/CBS level of theory are available for 34 of the possible 36 complexes that can be obtained by combination of 6 Lewis bases (OC, HCN, H$_2$O, H$_3$N, H$_2$S and PH$_3$) and 6 Lewis acids (LiF, LiH, LiCH$_3$, NaF, NaH and NaCH$_3$). We have shown elsewhere [28,29] that D_e can be partitioned between the Lewis base B and the

Lewis acid A in complexes B···A to give quantities that are measures of the nucleophilicity N_B of B and the electrophilicity E_A of A.

The simultaneous fitting of the N_B and E_A values (pure numbers) to the dissociation energies of the 34 complexes was carried out by means of Equation (1).

$$D_e = c \cdot \left(\sum_{i=1}^{6} x_i \cdot N_{B_i} \right) \cdot \left(\sum_{j=1}^{6} x_j \cdot E_{A_j} \right) \tag{1}$$

where the constant c has a value of 1.00 kJ mol^{-1} to ensure identical units on both sides of the equation. The x_i and x_j are parameters which have the value of 1.0 if the corresponding molecule is present in the complex and 0.0 otherwise. The resulting values of N_B and E_A so determined are set out in Table 3, while the observed and calculated values of D_e, and the residuals of the fit are included as Table S4 of the Supplementary Material. Clearly, the N_B and E_A are well determined, as indicated by the graph of D_e(*ab initio*) versus D_e(fitted) shown in Figure S1 of the Supplementary Material which is included with Table S4 and the value of $R^2 = 0.996$ for the linear regression fit shown in Figure S1. The relationship between D_e, N_B and E_A is easily visualized by means of Figure 6, in which D_e is plotted against the fitted N_B values of the six Lewis bases CO, HCN, H_2O, NH_3, H_2S and PH_3. For each series B···LiR and B···NaR (Type
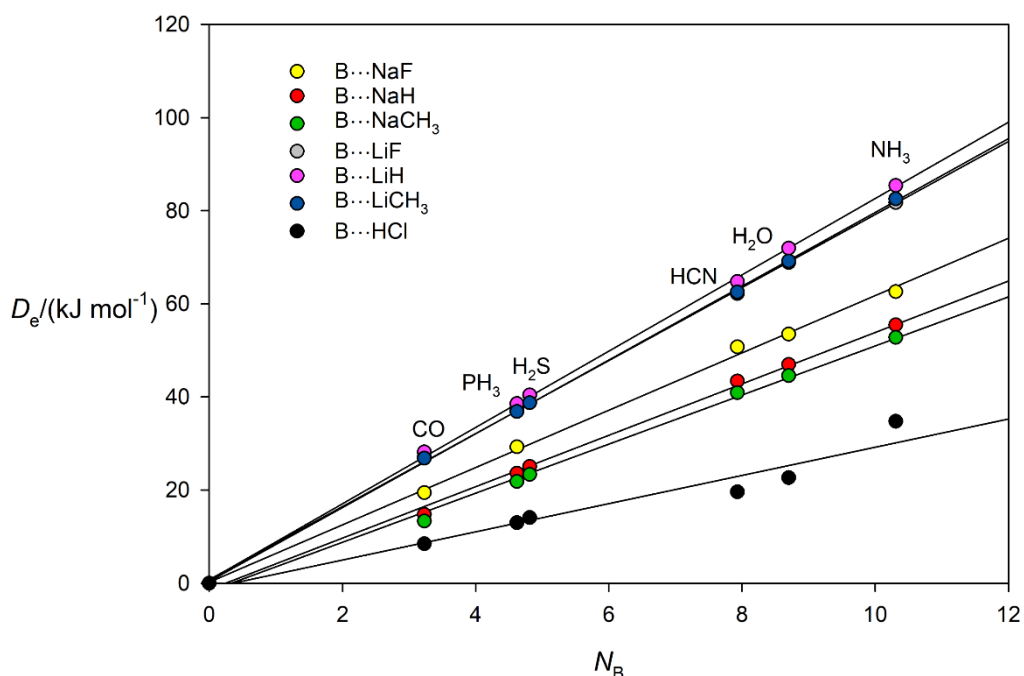
I complexes only), the points lie on a good straight line through the origin.

Figure 6. Plots of D_e versus N_B for Type I complexes in the series B···LiR and B···NaR, when R = F, H and CH₃ and B = CO, HCN, H_2O, NH_3, H_2S and PH_3. Values of N_B are given in Table 1.

The gradient of each line is the E_A value of the Lewis acid. It is clear from Figure 6 that LiF, LiH and LiCH$_3$ have almost the same electrophilicity. The order is $E_{LiH} \gtrsim E_{LiF} = E_{LiCH3}$; indeed the points for LiF are obscured by those of LiCH$_3$ in Figure 6. On the other hand, the order of electrophilicities among the NaR molecules is $E_{NaF} > E_{NaH} \approx E_{NaCH3}$. In terms of the inductive effect of the groups F and CH$_3$ relative to H, the –I effect of F is larger than the +I effect of CH$_3$ in NaR, but these effects appear to be negligible in the LiR, possibly because Li is less polarizable than Na and therefore induction effects are smaller in the B···LiR. The N_B values fitted for these complexes differ significantly from those found for hydrogen- and halogen-bonded complexes for a given Lewis base [29]. This could indicate a different nature of the

interactions in alkali-metal complexes compared with their hydrogen-and halogen-bonded bond analogues, which is the topic of the next sub-section.

3.4 Analysis of SAPT calculations for B⋯LiR and B⋯NaR

A SAPT analysis was carried out to investigate the non-covalent interactions in the B⋯LiR and B⋯NaR complexes (R = F, H and CH_3) for each of the six Lewis bases B =OC, HCN, H_2O, H_3N, H_2S and PH_3. The calculations were executed at the SAPT2+(3)δMP2 level, using the awCVTZ basis defined above. In order to compare these alkali-metal bonds with hydrogen and halogen bonds, SAPT calculations at the same level of theory were conducted on B⋯HCl and B⋯ClF complexes involving the same set of B. Figure 7 summarises a comparison of the SAPT-derived composition of the interactions in the complexes in which the non-covalent
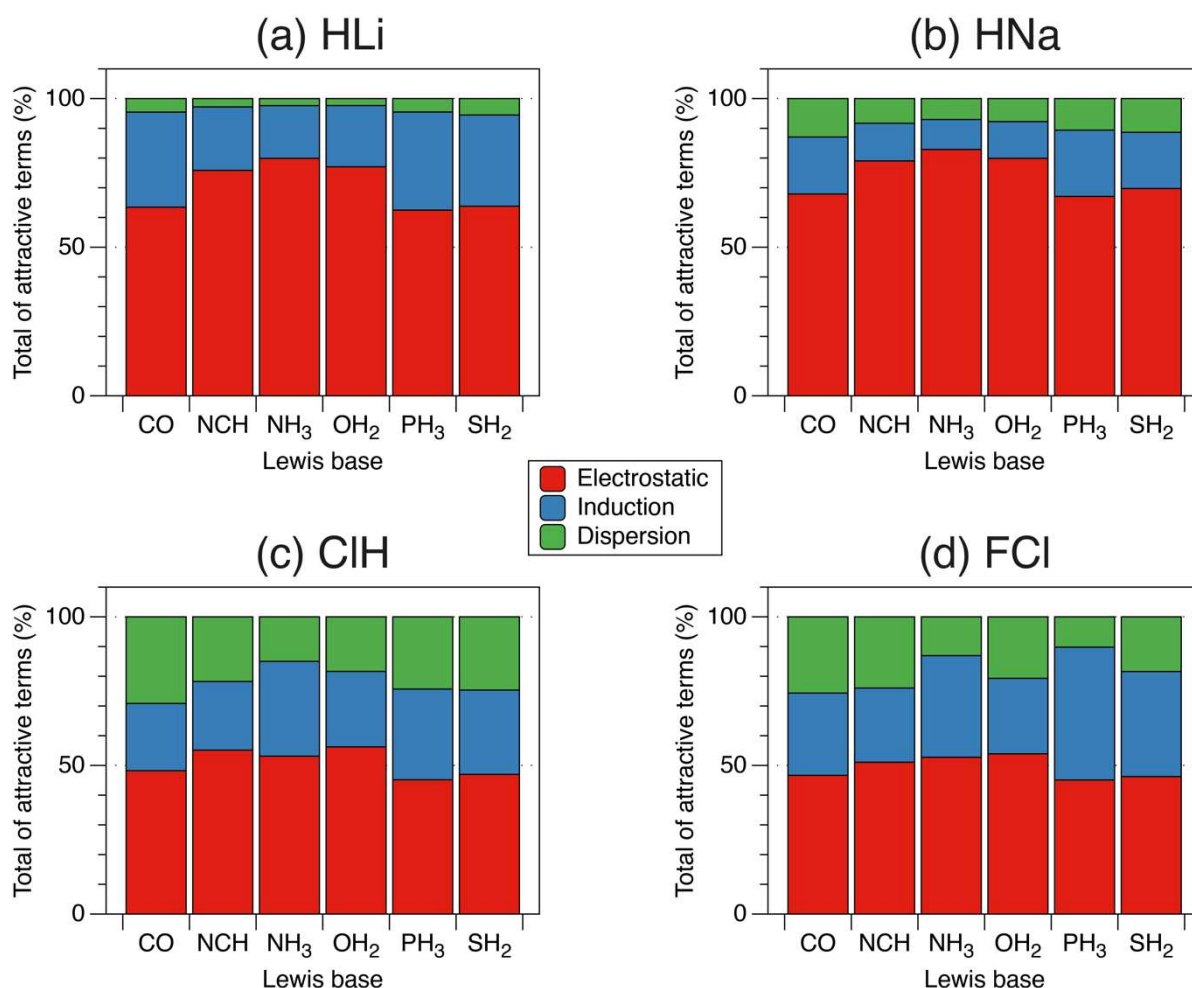
Figure 7. A comparison of the SAPT-derived composition of the interactions in the lithium-bonded complexes B⋯LiR and B⋯NaR (R= F, H and CH_3) for the indicated 6 Lewis bases B with that of the corresponding hydrogen-bonded and halogen-boned complexes B⋯HCl and B⋯ClF. Each term is shown as a percentage of the sum of the attractive terms (electrostatic, induction and dispersion). Exchange repulsion is not included.

interaction is via (a) a lithium-bond, (b) a sodium bond, (c) a hydrogen bond and (d) a halogen bond. Each term is shown as a percentage of the total attractive terms (electrostatic, induction and dispersion) in an attempt to normalise the values. The (repulsive) exchange term is excluded, and any charge transfer would be incorporated into the induction term.

Clearly, both the lithium and sodium bonds are more electrostatic in nature than the corresponding hydrogen and halogen bonds. Lithium bonds have an almost negligible dispersion contribution (presumably because of the low polarisability of lithium), while for sodium bonds both the induction and dispersion terms are small percentages compared to hydrogen / halogen bonds. Note that the Lewis bases HCN, NH_3 and H_2O all have significant increases in importance of the electrostatic term for the lithium and sodium bonds (this is also evident, but to a much smaller extent for the hydrogen and halogen bonds).

Figure 8 shows the SAPT electrostatic term (E_{elec}), in "raw" energetic form, for the complexes B···M–R plotted against the numerical nucleophilicities (N_B) for the Lewis bases derived from the simple model. For a given Lewis base, there is clear clustering of E_{elec} for both the lithium and sodium containing complexes, with the lithium containing species producing a larger electrostatic contribution. This reflects the larger electrophilicity values assigned to the lithium species, and the electrostatic ordering also generally matches the ordering of E_A. For example, LiH has the largest E_A and its complexes have the largest electrostatic contribution for a given Lewis base. It can also be seen that as the value of N_B increases, the electrostatic contribution to the total interaction energy also increases, although the relationship appears closer to quadratic, rather than linear, in nature. These results reinforce the finding that the non-covalent interactions in the lithium and sodium complexes are primarily electrostatic in nature, and that the E_A and N_B model parameters are encapsulating vital information about the underlying nature of the interactions.
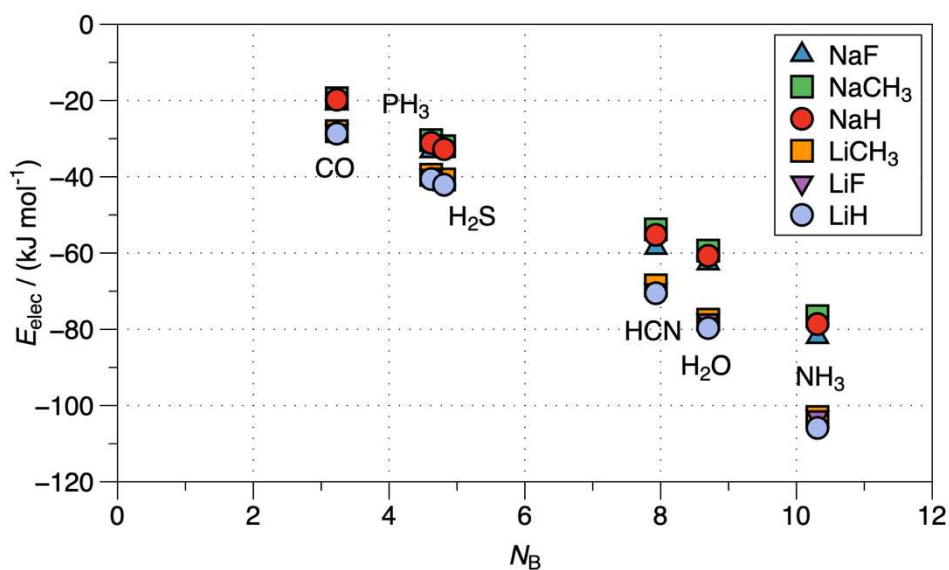
Figure 8. Relationship between the SAPT electrostatic term (E_{elec}) for the series of Type I complexes B···LiR and B···NaR (R= F, H and CH_3) and the numerical nucleophilicities (N_B) assigned to the 6 indicated Lewis bases B.

3.5 Analysis of differences between Type I and Type II complexes.

It is clear from Section 3.1 that when lower-energy, Type II B···NaR complexes exist, there is strong evidence of a secondary interaction between H atoms of the Lewis base and either F or H of NaR, as confirmed by an AIM analysis (see Figure S2 of the Supplementary Material). Dissociation energies for the Type II complexes were calculated at the CCSD(T)/CBS level, with the Na 2s2p correlated, and are given in Table 4. A comparison of the Type II dissociation energies with the Type I equivalents in Table 2 shows no consistent trend in complex stability; for H_3P···NaF the Type II D_e is only 1.4 kJ mol^{-1} larger than that for the Type I local minima, but this difference reaches a maximum of over 41 kJ mol^{-1} for H_2O···NaF. A SAPT analysis comparing the interactions was also carried out, using the same methodology as detailed above, with absolute values of the SAPT terms presented in the Supporting Information (see Tables S6-S8). Figure 9 summarises the comparison of the interaction in which the complex is (a) Type I, or (b) Type II. As in Figure 7, each term is shown as a percentage of the total attractive terms.
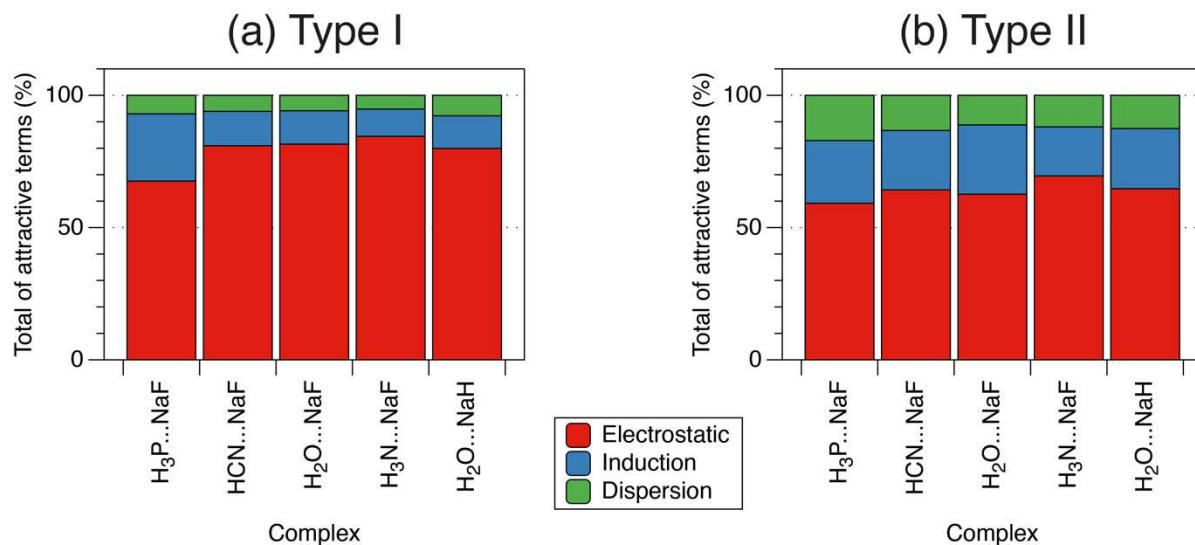
Figure 9. A comparison of the SAPT derived composition of the interactions in the complexes B···NaR (R = F or H) where both Type I and Type II complexes have been located. Each term is shown as a percentage of the sum of the attractive terms (electrostatic, induction and dispersion). Exchange repulsion is not included.

It is immediately obvious from Figure 9 that the underlying nature of the interaction in Type II complexes is significantly different to that of the analogous Type I complex. Although the electrostatic term remains the greatest attractive contribution to the interaction in all cases, it is substantially reduced in Type II complexes, while both induction and dispersion contributions increase. The SAPT charge transfer method (SAPT-CT) computes the charge transfer energy as the difference between the induction energies evaluated with dimer-centred and monomer-centred basis [47], and thus provides some additional insights into the nature of interactions between molecules. Table S5 in the Supporting Information compares the SAPT charge transfer terms for the Type I and Type II complexes, where it can be seen for Type I complexes that the charge transfer contribution is essentially negligible at less than 1 kJ mol^{-1}. However, the significance of charge transfer in Type II complexes is much less clear cut. For H$_3$P···NaF the charge transfer term is small at roughly –1 kJ mol^{-1}, although it should be noted that this is approximately equal to the additional stability of the Type II complex, and reaches a maximum of –18.24 kJ mol^{-1} for H$_2$O···NaF. This indicates that charge transfer plays an important role in the Type II complexes and their increased induction contribution, but it is not clear to what extent this contributes to the secondary interaction.

4.   Conclusions.

The aim of the work reported here was to investigate by *ab initio* calculations of benchmark quality the non-covalent interactions of simple molecules containing one of the alkali metal atoms Li or Na with a set of simple Lewis bases. To this end, the geometries, equilibrium dissociation energies D_e^{CBS} and intermolecular stretching force constants k_σ were evaluated for two series of complexes B···LiR and B···NaR, where R is F, H or CH_3 and the Lewis bases B are CO, PH_3, H_2S, HCN, H_2O or NH_3. The choice of the three simple groups R was made in order to ascertain the effects of the different inductive effects of F, H and CH_3 on the properties determined, given the generally accepted $-I$ effect of F and the $+I$ effect of CH_3 relative to H.

It was discovered from the geometry optimisations that for the complexes B···LiR there was only one energy minimum (with the two exceptions of H_2O···LiH and H_2S···LiF which exhibited two and no minima, respectively). The geometries at these minima were shown to be isomorphous with those of the corresponding hydrogen-bonded complexes B···HF and hence to obey the simple rules [6] for the prediction of hydrogen-bond angular geometries. In most of the complexes B···NaH and B···NaF two minima were found. The geometry at the lower energy minimum in such cases showed evidence of not only a primary interaction of the electrophilic Na atom with the nucleophilic non-bonding electron pair of the Lewis base B (*i.e.* an alkali metal bond), but also a significant secondary interaction involving the nucleophilic part of NaR with the more electrophilic region of B. Complexes of NaR and LiR that are isomorphous with the B···HF series are labelled Type I complexes while those of lower energy and displaying significant secondary interactions are named Type II.

For Type I complexes B···LiR and B···NaR, a direct proportionality was established between the two measures of binding strength D_e^{CBS} and k_α. Moreover, the gradient of the linear regression fit through the origin for these alkali-metal complexes is identical (within the fitting error) with that for B···HX (X =F, Cl, Br). As for the hydrogen-bonded series, it has been possible to express the D_e^{CBS} for the complexes B···LiR and B···NaR as the simple product of an electrophilicity E_A assigned to LiR or NaR and the nucleophilicity N_B of the Lewis base B. Moreover, plots of D_e^{CBS} versus N_B show that the electrophilicities of the LiR are nearly independent of the group R and lie in the order $E_{LiH} \gtrsim E_{LiF} = E_{LiCH3}$. The order $E_{NaF} > E_{NaH} \approx E_{NaCH3}$ found for the NaR is consistent with an inductive effect $-I$ for F that is larger in

magnitude than the +I effect of CH_3, both relative to H. The larger E_A values for the three LiR molecules than their NaR analogues and their near equality seems likely to result from the fact that Li^+ has only a $1s^2$ core which is smaller than that $(1s^2, 2s^2, 2p^6)$ of Na^+ and can therefore approach the Lewis base more closely.

A SAPT analysis carried out to investigate the nature of non-covalent interactions in the B···LiH and B···NaH complexes (R = F, H and CH_3) for each of the six Lewis bases B = OC, HCN, H_2O, H_3N, H_2S and PH_3 concludes that the non-covalent interaction involved is primarily electrostatic in nature. Comparison with the results of a similar analysis for the analogous hydrogen-bonded B···HCl and the halogen-bonded B···ClF species demonstrate that the LiH and NaH complexes have a larger electrostatic contribution to D_e^{CBS} than do their hydrogen- and halogen-bonded counterparts. The SAPT results reflect the conclusion from the N_B and E_A analysis that the ability to form predominantly electrostatic, non-covalent, alkali-metal bonds bonds lies in the order LiR > NaR, The smaller polarizability of Li^+ than of Na^+ is probably responsible for the smaller dispersion contribution to the energies obtained for the B···LiR.

5. Acknowledgements.

6. References

1. Polarity and ionization from the standpoint of the Lewis theory of valence. W. M. Latimer and W. H. Rodebush, *J. Am. Chem. Soc.* **42**, 1419-1433 (1920).
2. Definition of the hydrogen bond (IUPAC Recommendations 2011), E. Arunan, G. R. Desiraju, R. A. Klein, J. Sadlej, S. Scheiner, I. Alkorta, D. C. Clary, R. H. Crabtree, J. J. Dannenberg, P. Hobza, H. G. Kjaergaard, A. C. Legon, B. Mennucci, and D. J. Nesbitt, *Pure Appl. Chem.*, **83**, 1637-1641 (2011).
3. Definition of the halogen bond (IUPAC Recommendations 2013). G. R. Desiraju, P. S. Ho, L. Kloo, A. C. Legon, R. Marquardt, P. Metrangolo, P. A. Politzer, G. Resnati and K. Rissanen, *Pure Appl. Chemistry,* **85**, 1711-1713, (2013).

4. Definition of the chalcogen bond (IUPAC Recommendations 2019). C. B. Aakeroy, D. L. Bryce, G. R. Desiraju, A. Frontera, A. C. Legon, F. Nicotra, K. Rissanen, S. Scheiner, G. Terraneo, P. Metrangolo and G. Resnati, *Pure Appl. Chem*. 92, 1899-1892, (2019).

5. What's in a name? 'Coinage-metal' non-covalent bonds and their definition. A. C. Legon and N. R. Walker, *Phys. Chem. Chem. Phys*., **20**, 19332-19338 (2018).

6. Determination of properties of hydrogen-bonded dimers by rotational spectroscopy and a classification of dimer geometries. A. C. Legon and D. J. Millen, *Faraday Discuss. Chem. Soc.*, **73,** 71-87, (1982).

7. Angular geometries and other properties of hydrogen-bonded dimers: a simple electrostatic interpretation based on the success of the electron-pair model, A. C. Legon and D. J. Millen, *Chem. Soc. Reviews*, **16**, 467-498 (1987).

8. Do electrostatic interactions predict structures of van der Waals molecules? A. D. Buckingham and P. W. Fowler, *J. Chem. Phys*., **79**, 6426-6428 (1983).

9. Comments on ''Do electrostatic interactions predict structures of van der Waals molecules?'' F. A. Baiocchi, W. Reiher, and W. Klemperer, *J. Chem. Phys*., **79**, 6428-6429 (1983).

10. The lithium bond. P. A. Kollman, J. F. Liebman and L.C. Allen, *J Am. Chem. Soc*., **92**, 1142-1150, (1970).

11. Matrix isolation infrared studies of lithium bonding. B. S. Ault and G. C. Pimentel, *J. Phys. Chem.*, **79**, 621-626, (1975).

12. Comparison of lithium and hydrogen bonds. S. Scheiner, Chapter 3, p67-87 in 'Lithium Chemistry: A theoretical and experimental overview.' Editors A.-M. Sapse and P. von R. Schleyer, Wiley-Interscience, New York, 1995.

13. π-systems as lithium/hydrogen bond acceptors: Some theoretical observations. S. Salai Cheettu Ammal and P. Venuvanalingam, *J. Chem. Phys*.,**109**, 9820-9830, (2009).

14. Blue-shifted lithium bonds. Y. Feng, L. You, J. T. Wang, X. S. Li, and Q. S. Gou, *Chem. Commun*. 88-89, (2004).

15. Characterizing Complexes with F−Li···N, H−Li···N, and CH_3Li···N Lithium Bonds: Structures, Binding Energies, and Spin−Spin Coupling Constants. J. E. Del Bene, I. Alkorta, J. Elguero *J. Phys. Chem. A*, **113**, 10327–10334 (2009).

16. Ab Initio Study of Lithium-Bonded Complexes with Carbene as an Electron Donor. Q. Z. Li, H. Z. Wang,; Z. B. Liu, W. Z. Li, J. B. Cheng, B. A. Gong and J. Z. Sun, *J. Phys. Chem. A*, **113**, 14156-14160, (2009).

17. The single-electron hydrogen, lithium, and halogen bonds with HBe, H2B, and H3C radicals as the electron donor: an ab initio study. Q. Z. Li, R. Li, S. C. Yi, W. Z. Li and J. B. Cheng, *Struct. Chem*. **23**, 411-416, (2012).

18. Interplay and competition between the lithium bonding and halogen bonding: R_3C···XCN···LiCN and R_3C···LiCN···XCN as a working model (R = H, CH$_3$; X = Cl, Br). M. Solimannejad, Z. Rezaei and M. D. Esrafili, *Mol. Phys*., **112**, 1783-1788, (2014).

19. Enhancement effect of lithium bonding on the strength of pnicogen bonds: XH_2P···NCLi···NCY as a working model (X = F, Cl; Y = H, F, Cl, CN). M. Solimannejad, E. Bayati and M. D. Esrafili, *Mol. Phys*., **112**, 2058-2062, (2014).

20. Hydrogen bonding, halogen bonding and lithium bonding: an atoms in molecules and natural bond orbital perspective towards conservation of total bond order, inter- and intra-molecular bonding. A. Shahi and E. Arunan, *Phys. Chem. Chem. Phys*. **16**, 22935-22952, (2014).

21. Strengthening halogen. halogen interactions by hydrogen and lithium bonds in NCM···NCX···YCH$_3$ and CNM···CNX···YCH$_3$ (M = H, Li and X, Y = Cl, Br) complexes: a comparative study. M. D. Esrafili and M. Vakili, *Mol. Phys*., **114**, 325-332, (2016).

22. The B-C and C-C bonds as preferred electron source for H-bond and Li-bond interactions in complex pairing of $C_4B_2H_6$ with HF and LiH molecules. A. Zabardasti, N. Talebi, A. Kakanejadifard and Z. Saki, *Struct. Chem*., **27**, 573-581, (2016).

23. Comparison of the directionality of the halogen, hydrogen, and lithium bonds between HOOOH and XF (X = Cl, Br, H, Li). L. X. Liu, L. P. Meng, X.Y. Zhang, and Y. L. Zeng, *J. Mol. Model*., **22**, Article 52, (2016).

24. The influence of hydrogen- and lithium-bonding on the cooperativity of chalcogen bonds: A comparative ab initio study. M. D. Esrafili, P. Mousavian and F. Mohammadian-Sabet, *Mol. Phys*. **117**, 726-733, (2019).

25. Microwave Spectroscopy. C. H. Townes and A. L. Schawlow, McGraw-Hill, New York, 1955, Chapter 9, p236.

26. A fifth-order perturbation comparison of electron correlation theories. K. Raghavachari, G.W. Trucks, J.A. Pople and M. Head-Gordon, *Chem. Phys. Lett*., **157**, 479-483 (1989).

27. Structure and Mechanism in Organic Chemistry, C. K. Ingold, Cornell University Press, Ithaca, New York, 1953, Chapter 2, p67-73.

28. A reduced radial potential energy function for the halogen bond and the hydrogen bond in complexes B···XY and B···HX, where X and Y are halogen atoms, A. C. Legon, *Phys. Chem. Chem. Phys.*, **16**, 12415-12421 (2014). Correction: **16**, 25199-25199, (2014).

29. Nucleophilicities of Lewis bases B and electrophilicities of Lewis acids as determined from the dissociation energies of complexes B···A involving hydrogen bonds, tetrel bonds, pnictogen bonds, chalcogen bonds and halogen bonds. I. Alkorta and A. C. Legon, *Molecules*, **22**, 1786-1799 (2017).

30. Gaussian basis sets for use in correlated molecular calculations. I. The atoms boron through neon and hydrogen. T.H. Dunning, Jr., *J. Chem. Phys*. **90**, 1007-1023 (1989).

31. Electron affinities of the first-row atoms revisited. Systematic basis sets and wave functions. R.A. Kendall, T.H. Dunning, Jr. and R.J. Harrison, *J. Chem. Phys.*, **96**, 6796-6806 (1992).

32. Gaussian basis sets for use in correlated molecular calculations. III. The second row atoms Al-Ar. D.E. Woon and T.H. Dunning, Jr., *J. Chem. Phys*. **98**, 1358-1371 (1993).

33. Gaussian basis sets for use in correlated molecular calculations. VII. Valence, core-valence, and scalar relativistic basis sets for Li, Be, Na, and Mg. B. P. Prascher, D. E. Woon, K. A. Peterson, T. H. Dunning, Jr. and A. K. Wilson *Theor. Chem. Acc.*, **128**, 69–82 (2011).

34. Application of systematic sequences of wave functions to the water dimer. D. Feller, *J. Chem. Phys.* **96**, 6104-6114 (1992).

35. Werner, H.-J.; Knowles, P. J.; Knizia, G.; Manby, F. R.; Schütz, M.; Celani, P.; Györffy, W.; Kats, D.; Korona, T.; Lindh, R.; Mitrushenkov, A.; Rauhut, G.; Shamasundar, K. R.; Adler, T. B.; Amos, R. D.; Bernhardsson, A.; Berning, A.; Cooper, D. L.; Deegan, M. J. O.; Dobbyn, A. J.; Eckert, F.; Goll, E.; Hampel, C.; Hesselmann, A.; Hetzer, G.; Hrenar, T.; Jansen, G.; Köppl, C.; Liu, Y.; Lloyd, A. W.; Mata, R. A.; May, A. J.; McNicholas, S. J.; Meyer, W.; Mura, M. E.; Nicklass, A.; O'Neill, D. P.; Palmieri, P.; Peng, D.; Pflüger, K.; Pitzer, R.; Reiher, M.; Shiozaki, T.; Stoll, H.; Stone, A. J.; Tarroni, R.; Thorsteinsson, T.; Wang, M. Molpro, Version 2012.1, a Package of Ab Initio Programs.

36. Ab initio study of the alkali and alkaline-earth monohydroxides. C. W. Bauschlicher and S. R. Langhoff, *J. Chem. Phys*. **84**, 901-909 (1986).

37. Pair natural orbital and canonical coupled cluster reaction enthalpies involving light to heavy alkali and alkaline earth metals: the importance of sub-valence correlation. Y. Minenkov, G. Bistoni, C. Riplinger, A. A. Auer, F. Neese and L. Cavallo*, Phys. Chem. Chem .Phys.*, **19**, 9374-9391 (2017).

38. Gaussian basis sets for use in correlated molecular calculations. XI. Pseudopotential-based and all-electron relativistic basis sets for alkali metal (K–Fr) and alkaline earth (Ca–Ra) elements. J. G. Hill and K. A. Petersen, *J. Chem. Phys*. **147**, 244106 (2017).

39. Gaussian basis sets for use in correlated molecular calculations. X. The atoms aluminum through argon revisited. T. H. Dunning, Jr., K. A. Peterson, and A. K. Wilson, *J. Chem. Phys*. **114**, 9244-9253 (2001).

40. Psi4 1.1: An Open-Source Electronic Structure Program Emphasizing Automation, Advanced Libraries, and Interoperability. R. M Parrish, L. A. Burns, D. G. A. Smith, A. C. Simmonett, A. E. DePrince III, E. G. Hohenstein, U. Bozkaya, A. Y. Sokolov, R. Di Remigio, R. M. Richard, J. F. Gonthier, A. M. James, H. R. McAlexander, A. Kumar, M. Saitow, X. Wang, B. P. Pritchard, P. Verma, H. F. Schaefer III, K. Patkowski, R.A.King, E. F. Valeev, F. A. Evangelista, J. M.Turney, T. D. Crawford , and C. D. Sherrill. *J. Chem Theory Comput*. **13**, 3185-3197 (2017).

41. Perturbation Theory Approach to Intermolecular Potential Energy Surfaces of van der Waals Complexes. B. Jeziorski, R. Moszynski, and K. Szalewicz, *Chem. Rev.* **94**, 1887-1930 (1994).

42. Wavefunction methods for noncovalent interactions. E. G. Hohenstein and C. D. Sherrill, *WIREs Comput. Mol. Sci.*, **2**, 304–326 (2012).

43. Levels of symmetry adapted perturbation theory (SAPT). I. Efficiency and performance for interaction energies. T. M. Parker, L. A. Burns, R. M. Parrish, A. G. Ryno, and C. D. Sherrill, *J. Chem. Phys.,* **140**, 094106 (2014).

44. Density fitting of intramonomer correlation effects in symmetry-adapted perturbation theory. E. G. Hohenstein and C. D. Sherrill, *J. Chem. Phys*. **133**, 014101 (2010).

45. Spectroscopic investigations of hydrogen bonding interactions in the gas phase.   VII.   The equilibrium conformation and out-of-plane bending potential energy function of the hydrogen-bonded heterodimer H2O···HF determined from its microwave rotational spectrum, Z. Kisiel, A. C. Legon and D. J. Millen, *Proc. Roy. Soc. Lond. A*, **381**, 419-42, (1982).

46. Dihydrogen bonds (A-H···H-B). I. Alkorta, J. Elguero, C. Foces-Foces, *Chem. Commun.*, 1633-1634, (1996).

47. Charge-transfer in Symmetry-Adapted Perturbation Theory. A. J. Stone and A. J. Misquitta, *Chem. Phys. Lett*., **473**, 201-205 (2009).

Tables

Table 1. Values of D_e(CBS) and k_σ calculated for complexes B···LiR[a]

Complex	CCSD(T)/AVTZ	
	D_e(CBS)/(kJ mol^{-1})	k_σ/(N m^{-1})
OC···LiF	27.11	23.07
H$_3$P···LiF	37.49	23.36
H$_2$S···LiF	…	…
HCN···LiF	62.22	45.21
H$_2$O···LiF	68.87	52.63
H$_3$N···LiF	81.76	51.28
OC···LiH	28.15	22.60
H$_3$P···LiH	38.56	23.26
H$_2$S···LiH	40.39	24.59
HCN···LiH	64.77	44.88
H$_2$O···LiH	71.95	54.23
H$_3$N···LiH	85.43	52.40
OC···LiCH$_3$	26.82	22.56
H$_3$P···LiCH$_3$	36.84	22.78
H$_2$S···LiCH$_3$	38.74	24.17
HCN···LiCH$_3$	62.54	43.83
H$_2$O···LiCH$_3$	69.16	52.69
H$_3$N···LiCH$_3$	82.55	51.40

[a]These complexes have geometries that are isomorphous with those of the corresponding B···HF complexes (Type I) and are sometimes secondary minima found during the optimization process (see text)

Table 2. Values of D_e(CBS) and k_σ calculated for Type I complexes B···NaR with different basis sets for Na[a]

Complex	CCSD(T)/AVTZ		CCSD(T)/awCVTZ	
	D_e(CBS)/(kJ mol^{-1})	k_σ/(N m^{-1})	D_e(CBS)/(kJ mol^{-1})	k_σ/(N m^{-1})
OC···NaF	16.90	12.98	19.44	14.02
H$_3$P···NaF	26.87	13.96	29.25	15.71
H$_2$S···NaF	…	…	…	…
HCN···NaF	48.05	26.94	50.74	29.62
H$_2$O···NaF	46.42	38.02	53.48	34.30
H$_3$N···NaF	58.82	30.53	62.63	32.80
OC···NaH	13.90	10.38	14.75	10.64
H$_3$P···NaH	22.90	11.91	23.60	12.89
H$_2$S···NaH	24.00	12.71	25.06	13.65
HCN···NaH	42.62	24.16	43.38	25.54
H$_2$O···NaH	42.11	34.82	46.97	31.02
H$_3$N···NaH	53.99	28.58	55.50	29.77
OC···NaCH$_3$	12.74	9.66	13.31	9.88
H$_3$P···NaCH$_3$	21.50	11.27	21.81	12.20
H$_2$S···NaCH$_3$	22.63	12.02	23.32	13.02
HCN···NaCH$_3$	40.71	23.19	40.90	24.45
H$_2$O···NaCH$_3$	39.59	33.66	44.57	29.79
H$_3$N···NaCH$_3$	51.83	27.64	52.76	28.79

[a]These complexes have geometries that are isomorphous with those of the corresponding B···HF complexes and are sometimes secondary minima found during the optimization process (see text).

Table 3. Values of nucleophilicities N_B of six Lewis bases B and electrophilicities E_A of six Lewis acids MR (M= Li or Na, R = F, H, or CH$_3$) obtained by fitting D_e values using Eq.(1)

Lewis base B	N_B	Lewis acid A	E_A
OC	3.23	LiF	7.94
H$_3$P	4.62	LiH	8.29
H$_2$S	4.81	LiCH$_3$	7.98
HCN	7.93	NaF	6.19
H$_2$O	8.70	NaH	5.34
H$_3$N	10.31	NaCH$_3$	5.04

Table 4. Values of D_e(CBS)[a] calculated for Type II complexes B···NaR

Complex	D_e / (kJ mol^{-1})
H$_3$P···NaF	30.68
HCN···NaF	68.04
H$_2$O···NaF	95.15
H$_3$N···NaF	78.32
H$_2$O···NaH	63.36

[a] Calculated using the CCSD(T)/CBS (awCVnZ) basis sets.